J Solid State Electrochem (2003) 7: 599–606
DOI 10.1007/s10008-003-0362-3

ORIGINAL PAPER

Ana Prieto · Javier Hernández · Enrique Herrero
Juan M. Feliu

The role of anions in oxygen reduction in neutral and basic media on gold single-crystal electrodes

Received: 31 October 2002 / Accepted: 6 February 2003 / Published online: 1 July 2003
© Springer-Verlag 2003

Abstract Oxygen reduction on well-defined single-crystal electrodes in different basic and neutral media has been studied using the impinging jet system. The results obtained with this system in 0.1 M NaOH are comparable to those reported in the literature for rotating disk electrodes, indicating that the impinging jet system behaves as a system in which the thickness of the diffusion layer is stationary. The activity of the Au(100) electrode is considerably higher than the rest of the basal planes in all media and yields water when $E > -0.2$ V and hydrogen peroxide for $E < -0.2$ V on the SHE scale. For Au(111) and Au(110) the activity of the electrode is much smaller and the final product is always hydrogen peroxide. The transition between both mechanisms for the Au(100) is, essentially, independent of the solution pH. In acid media the final product is always hydrogen peroxide for all the electrodes studied. The differences between the activities of the electrodes have been explained in the light of the different adsorption properties of the surfaces in relation to HO_2^-. In the case of the Au(100) electrode, the existence of a negative charge density on the metal inhibits further reduction of HO_2^-.

Keywords Basic media · Gold electrodes · Impinging jet system · Oxygen reduction · Single-crystal electrodes

Introduction

Oxygen reduction is one of the most important electrochemical reactions since it has multiple applications in a variety of research fields, ranging from energy conversion to corrosion science. Therefore, understanding the nature of the electrocatalytic process of oxygen reduction has been the subject of a vast number of works. Although the knowledge of the oxygen reduction process has advanced considerably in recent years [1, 2, 3, 4], there are many aspects of the kinetics of this heterogeneous reaction that are not fully understood.

The nature and surface structure of the electrode is a fundamental aspect to consider when one or several intermediates can be adsorbed on the electrode surface. This is especially the case for oxygen reduction, in which four electrons are involved in the final reduction to water. The high number of electrons exchanged per oxygen molecule would imply the possible existence of several adsorption intermediates, whose interaction energy with the surface will depend on the metal and its surface structure. It is well known that platinum exhibits the highest catalytic activity for the $4e^-$ pathway among the pure metals studied [4].

The substrate not only affects the catalytic activity but also the final product of the reaction and the mechanism. The general mechanism for oxygen reduction consists of two "interactive" parallel pathways, in which one leads to the formation of water (OH^- in basic media) with hydrogen peroxide (HO_2^- in basic media) as the intermediate species, and the second path yields water (OH^- in basic media) directly [5, 6]. Depending on the catalytic activity of the metal, the final product can be water (OH^-) or hydrogen peroxide. In these latter cases, further reduction of hydrogen peroxide is highly inhibited.

Oxygen reduction on gold single-crystal electrodes has been extensively studied both in acid and basic media [5, 6, 7, 8, 9, 10, 11, 12, 13, 14, 15]. Generally, the reaction only involves two electrons, yielding hydrogen peroxide as the final product, a clear indication that the only path operating for gold is via hydrogen peroxide. However, a four-electron reaction (OH^- is the final product) is observed for Au(100) and vicinal faces in NaOH media [9, 12]. The general scheme for the

Dedicated to Prof. Dr. Wolf Vielstich on the occasion of his 80th birthday in recognition of his numerous contributions to interfacial electrochemistry

A. Prieto · J. Hernández · E. Herrero · J. M. Feliu (✉)
Departamento Química Física, Universidad de Alicante,
Apdo. 99, 03080 Alicante, Spain
E-mail: juan.feliu@ua.es

reduction of oxygen [4] can be simplified for the case of Au(100) electrodes in basic media as a series mechanism [7] in which oxygen is first reduced to hydrogen peroxide and then this species is further reduced to OH^-:

$$O_2 + 2H^+ + 4e \rightleftharpoons 2OH^-$$

$$O_{2,b} \xrightarrow{dif} \boxed{O_{2,a} \xrightarrow{1e} O_{2,a}^-} \xleftrightarrow[H^*]{1e} HO_{2,a}^- \xleftrightarrow[H^*]{1e} O_a^- + OH^- \xleftrightarrow{1e} OH^- \qquad (1)$$

$$HO_{2,a}^- \updownarrow HO_{2,b}^-$$

where the subscripts a and b means adsorbed and bulk. This electrode also shows the highest catalytic activity of all basal planes and is similar to that obtained for platinum electrodes. Irrespective of the final product, a Tafel slope of 120 mV is always obtained, indicating that the first electron transfer is the rate-determining step. The differences between the Au(100) electrodes and the other Au single-crystal electrodes have been explained according to the different adsorption properties for OH, which is considered to catalyze both the reduction of oxygen and hydrogen peroxide [4].

The aim of this work is to study oxygen reduction on gold single-crystal electrodes in different media, by using the impinging jet system. The impinging jet system is a hydrodynamic technique [15], which maintains the diffusion layer constant with time. The use of different media at different pH values will serve to establish the role of the different species in the reduction mechanism.

Experimental

Gold single-crystal electrodes were obtained from small (ca. 2 mm diameter) single-crystal beads, in turn obtained by melting a 0.5 mm Au (99.99%, Goodfellow) wire. After careful cooling, the resulting single-crystal beads were oriented, cut and polished following the procedure described for Pt beads [16]. Prior to each experiment the single-crystal electrodes were flame-annealed and quenched with ultrapure water. A large gold counter-electrode (99.99%) and a reversible hydrogen electrode separated from the cell compartment were used. In order to compare the results obtained from different electrolytes, the potentials were changed to the SHE scale. All measurements were made at room temperature. Solutions were prepared from sulfuric acid (Merck Suprapur), sodium sulfate (Aldrich) and sodium hydroxide (Merck Suprapur), in Millipore water.

Single-crystal electrodes have been characterized by cyclic voltammetry in 0.1 M NaOH (Fig. 1). The peaks appearing at ca. 0.25 V (SHE) for the Au(100) and 0.32 V (SHE) for the Au(111) electrodes are due to the lifting of the reconstruction of the electrode [17]. The highest peaks are obtained in the first cycle, since the electrode after the flame treatment is well reconstructed. The peaks diminish upon cycling, due to the fact that the reconstruction process, which takes place at negative potentials with respect to the peak, is a slow process.

Oxygen reduction experiments have been carried out by using the impinging jet system, as described [15]. In this system, a continuous electrolyte flow coming from a capillary is continuously replenishing the meniscus solution. This capillary is connected to two electrolyte containers through a computer-operated valve, which allows the selection of the electrolyte. For these experiments, both containers had the same electrolyte, one completely deoxygenated by continuous Ar bubbling and the other saturated with oxygen at atmospheric pressure. The experimental protocol is as

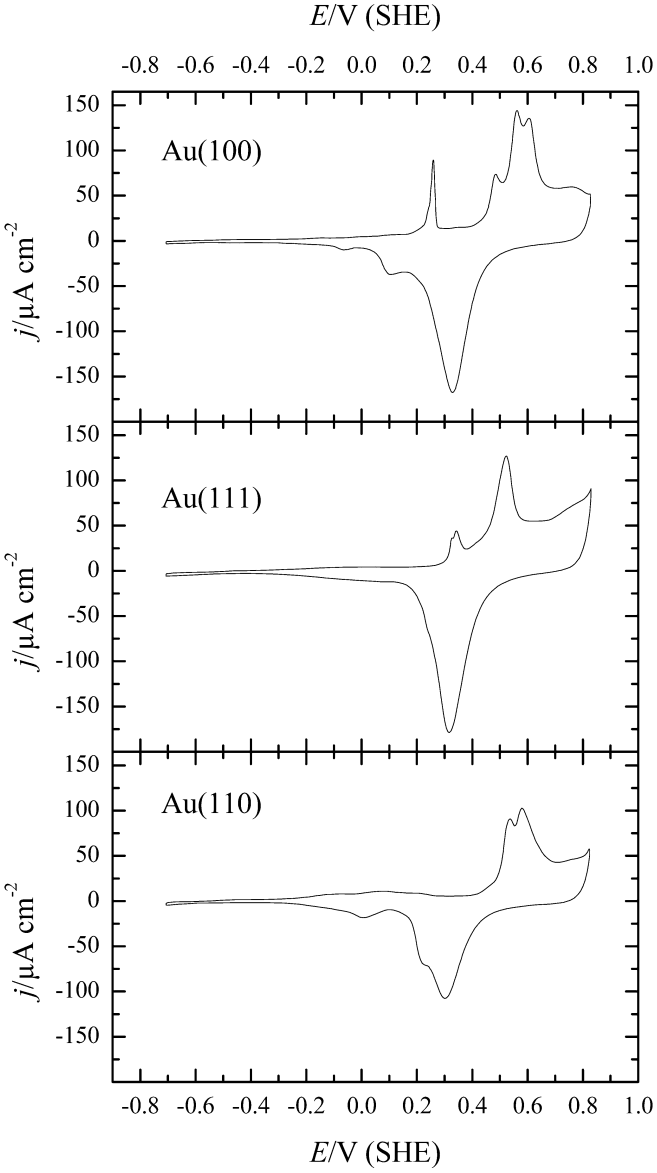

Fig. 1 Cyclic voltammogram (first cycle) of the Au(100), Au(111) and Au(110) electrodes in 0.1 M NaOH (scan rate 50 mV/s)

follows. Initially, the flow in the meniscus is coming from the deoxygenated electrolyte. With this electrolyte, a cyclic voltammogram of the electrode is recorded in order to ensure the cleanliness of the solution. After that, the scan is stopped at the upper potential limit, and the flow changed to the oxygen-containing solution. Finally, the cyclic voltammogram for the oxygen reduction reaction at 50 mV/s is recorded.

Results and discussion

The first point to establish in this work is the dynamical properties of the impinging jet system. Owing to its hydrodynamic characteristics, in which the solution in the meniscus is continuously replenished, it can be expected that the system behaves as a system in which the thickness of the diffusion layer is time independent, i.e. similar to a rotating disk electrode (RDE). In order to check the validity of the hypothesis, the oxygen reduction curve for a Au(100) electrode in 0.1 M NaOH was recorded and compared with the literature data (Fig. 2). As can be seen, the results obtained for the impinging jet system agree well with the results obtained for a rotating disk Au(100) electrode [12]. Even the plateau region is better defined in the impinging jet system, probably as a result of the cleanliness of the system. The main difference is the value of the limiting current density obtained, which is inversely proportional to the thickness of the diffusion layer characteristic of each system. For the impinging jet system, the limiting currents depend on the flow rate of the electrolyte in the meniscus (which is fixed in the present configuration), whereas for the rotating disk it depends on the rotation rate. The maximum current obtained at 0.0 V vs. SHE in the impinging jet system is six times lower than that obtained for a rotating disk electrode at 400 rpm, indicating that, in the present conditions of the impinging jet system, the diffusion layer is, on average, about six times thicker than that obtained in the aforementioned rotating disk experiment. This means that the net flow of the different species in solution to the electrode surface is, on average, six times slower in the impinging jet system, which has an effect on the cleanliness of the surfaces. The thickness of the diffusion layer in the impinging jet system is probably not uniform throughout the surface. The results of the comparison indicate, however, that the impinging jet system can be regarded as a system with a time-independent diffusion layer. Additional evidence for this is that the currents obtained in the voltammetric profile are insensitive to the scan rate, for scan rates below 100 mV/s.

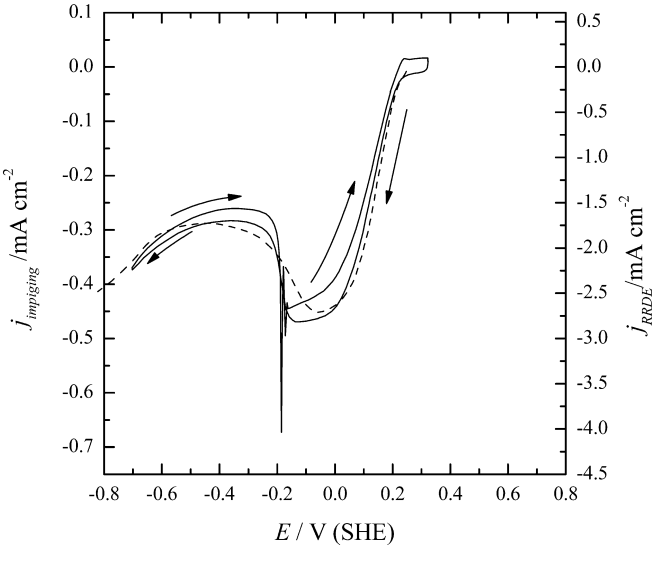

Fig. 2 Comparison of the current densities measured for oxygen reduction in the impinging jet system (*full line*, *left-hand axis*) and in a RRDE electrode (*dashed line*, *right-hand axis*, data obtained from [14]) in 0.1 M NaOH

Oxygen reduction on Au(100) electrodes in 0.1 M NaOH exhibits a unique behavior since it is the only gold basal plane that is able to yield OH^- as a final product of the oxygen reduction. At potentials above −0.2 V, the final product is OH^- [11] and a diffusion-limited current is found between 0.1 and 0.2 V. At potentials below −0.2 V, the current diminishes to almost half of the maximum value, yielding hydrogen peroxide as the final product [11]. The only significant difference with the previous results is the high amplitude of the oscillations in the positive-going scan at −0.2 V vs. SHE, where the transition between the two mechanisms takes place. It is well known that the observation of oscillations requires clean surfaces. The use of mild transport conditions in the impinging jet system will then favor the observations of oscillations, as stated above. A tentative explanation for these oscillations will be given below.

Since the formation of water as the final product is not observed in acid media [4], it is interesting to study how the pH affects the behavior of the gold electrodes. Figure 3 shows the voltammetric profiles for the oxygen reduction process in 0.1 M Na_2SO_4 (pH 6) for the three basal planes of gold. Although the pH of the interface is not well defined, it will be significantly more acidic than in 0.1 M NaOH. The three different profiles show the same characteristics found in 0.1 M NaOH. The most active plane is the (100), showing a voltammetric profile comparable to that found in 0.1 M NaOH. In this way, Au(100) should produce, at least partially, OH^- from oxygen reduction at this more acidic pH in the higher potential range (above −0.1 V) and hydrogen peroxide below this potential. As in the preceding electrolyte, oscillations are always present in the positive-going scan at ca. 0.1 V. Both Au(111) and Au(110) electrodes have much lower activity, as also happens in 0.1 M NaOH, and they probably only yield hydrogen peroxide, as reported from rotating ring disk electrode (RRDE) experiments in 0.1 M NaOH [10]. It is worth mentioning that the maximum currents for these later electrode surfaces are much lower than that obtained for the Au(100) electrode at potentials below −0.2 V, pointing out strong differences in the electrode activity that should be related to the surface structure.

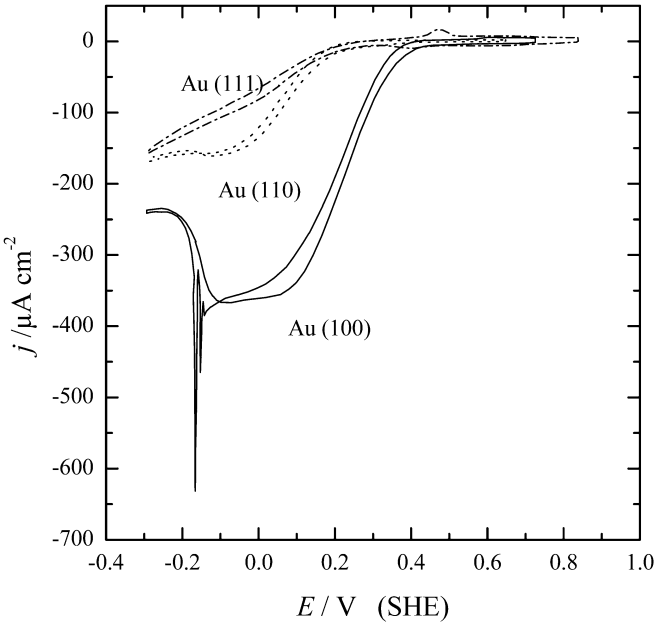

Fig. 3 Current densities measured for oxygen reduction in the impinging jet system in 0.1 M Na_2SO_4 (pH 6) for the Au(100), Au(111) and Au(110) electrodes

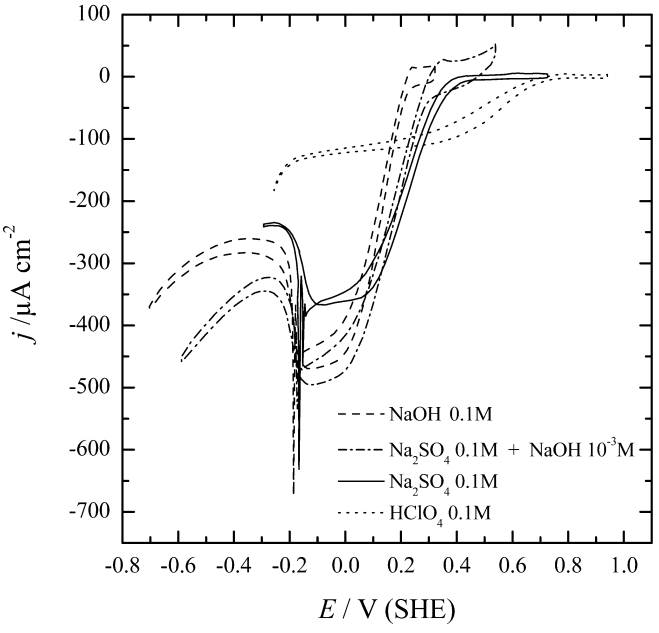

Fig. 4 Current densities measured for oxygen reduction in the impinging jet system in several electrolytes for the Au(100) electrode

When comparing the oxygen reduction curve in the two media (0.1 M NaOH and 0.1 M Na_2SO_4), it can be seen that the transition between the reduction mechanism with four electrons to that with two electrons takes place at constant potential (−0.2 V, SHE), independently of the pH of the solution. Similar results were observed with a Au(100) RDE [18]. It is worth noting that the pH in the interface in the case of the neutral sulfate solution may be different from that measured in the bulk, since two OH^- ions are generated per O_2 molecule in the four-electron reduction mechanism and the solution is not buffered. In the limiting case, when the limiting diffusion currents are attained, the pH in the interface might be as high as 11. However, this limiting pH value is significantly lower than that of 0.1 M NaOH solution. Several experiments in different electrolytes were also performed (Fig. 4), having the same general behavior. The onset of oxygen reduction shows some dependence on the pH and the maximum current decays at acid pH values. However, it is important to remark that the transition from the four-electron mechanism to the two-electron mechanism occurs at nearly the same electrode potential on the SHE scale. The small differences observed in the recorded plateau current are probably associated with small changes in the flow conditions induced by the exact meniscus position.

In acidic medium, the curves for oxygen reduction on Au(100) changes markedly. The currents obtained between 0.4 and 0.0 V are significantly smaller and do not show any transition between different products. Owing to the small currents obtained, the final product in acidic media should be hydrogen peroxide, in agreement with previous results [7, 12].

All these results can be summarized by considering that O_2 reduction is an irreversible process controlled simultaneously by the kinetics and the diffusion. In this case, the current is given by:

$$\frac{1}{j} = \frac{1}{j_{ex}} + \frac{1}{j_{dif}} \tag{2}$$

where j_{ex} is the current that would be obtained if the process were controlled by the kinetics of the electron transfer process and j_{dif} is the limiting diffusion current for the process. In order to obtain information about the kinetics of the electrode, the values of j_{ex} have to be extracted. Solving Eq. 2 for j_{ex}:

$$j_{ex} = \frac{j \times j_{dif}}{j_{dif} - j} \tag{3}$$

The values of j_{ex} were calculated for all the different curves using the current plateau measured at −0.15 V as the value for the limiting diffusion current. The Tafel plots constructed with the calculated j_{ex} values (Fig. 5) are linear in a wide potential range (over 0.4 V) and allow calculating the Tafel slope for the process. The values obtained for the Tafel slope are always in the range of 110–120 mV, which indicates that the first electron transfer is the rate-determining step. The wide range in which the Tafel plot is linear indicates that the process is well described by Eq. 2, i.e. it is simultaneously controlled by the kinetics and the diffusion and the current obtained at 0.2 V corresponds to the limiting diffusion current for the process.

Another important value, not usually calculated, that can be obtained from this representation is the apparent

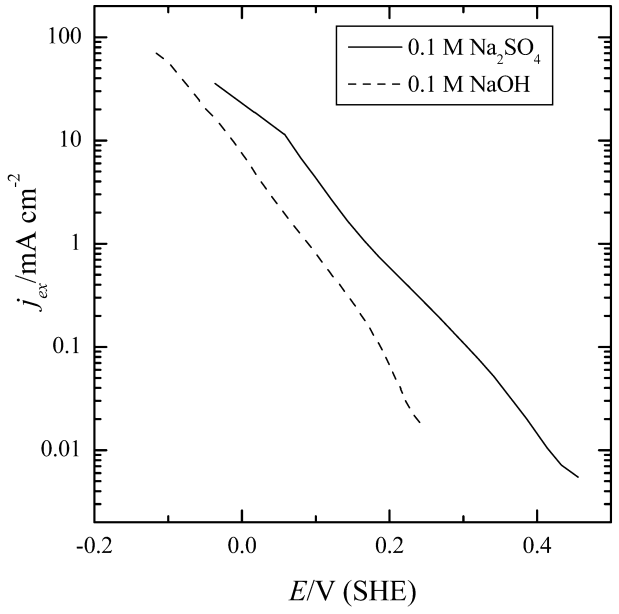

Fig. 5 Tafel plot for j_{ex} in 0.1 M NaOH and 0.1 M Na_2SO_4

order with respect to OH^-. The order can be evaluated from the current measured at a given potential as a function of the pH. For instance, the j_{ex} calculated at 0.1 V for 0.1 M NaOH is 0.8 mA cm^{-2}, whereas a value of 4.2 mA cm^{-2} is obtained in 0.1 M Na_2SO_4. Even in the case that the pH in the interface for this latter solution was 11, this would lead to a fractional order with respect to the OH^- of ca. $-1/3$. If the actual pH in the interface were lower, the order with respect to the OH^- would be even closer to zero. Such fractional order with respect to the OH^- concentration is difficult to explain according to the general scheme for oxygen reduction on gold [7]. The differences in the current and the position of the wave in this potential scale with respect to the pH can be explained by the different conditions of the electrode in the supporting electrolyte at different pH values, i.e. the different amount of anions adsorbed at a given potential in the different media. If this factor is taken into account, the order for the OH^- could be regarded as zero. This order represents a mean value for the whole pH interval studied.

The main qualitative difference for the Au(100) electrode compared with the rest of the basal planes of gold for oxygen reduction is the ability of this electrode to yield OH^- as a final product instead of hydrogen peroxide. When the reduction of hydrogen peroxide in 0.1 M NaOH is studied, only Au(100) shows significant reduction currents [7, 10]. For this electrode, reduction starts at 0.1 V (SHE) and increases until 0.2 V (SHE), where the current diminishes abruptly to zero. This behavior clearly indicates that the reduction of oxygen to OH^- only occurs in the region where hydrogen peroxide is readily reduced to OH^-. The difference in the behavior of the Au(100) electrode has been related to a higher amount of OH adsorbed on Au(100) with respect to the other orientations [14]. The adsorbed OH would catalyze the further reduction of the hydrogen peroxide formed, yielding OH^-. The transition between the two mechanisms was then associated with the potential at which the OH adsorption ends [14]. However, the results shown in Fig. 4 show no dependence of the transition with the pH, as would have been expected if adsorbed OH is implicated in the reduction of hydrogen peroxide to OH^-. Moreover, in 0.1 M Na_2SO_4, the most likely adsorbed species at the onset of oxygen reduction, in which the interfacial pH would have the same value as the solution pH, is sulfate [19]. Also, as Fig. 1 shows, the adsorption of OH also takes place on Au(111) and Au(110) electrodes in 0.1 M NaOH. Thus, the implication of OH in the reduction of hydrogen peroxide to OH^- on Au(100) seems dubious.

The transition between the two mechanisms (or the potential below which the electrode is unable to reduce hydrogen peroxide) should be then linked to a property of the surface that is pH independent. For gold single crystals, the position of the potential of zero charge (pzc) is almost independent of the pH, and the presence of sulfate on the solution only slightly shifts the pzc to more negative potentials [20]. Some processes on the electrode surface are associated with the position of the pzc. For Au(100) electrodes, the surface can undergo reconstruction, and this process is linked to the pzc. At potentials negative to the pzc, the stable phase is the reconstructed surface (a hexagonal phase), whereas at positive potentials the stable phase is the nominal (1×1) phase [21]. The lifting of the reconstruction is triggered by the positive charge [22], but the anions also play a role in this process [23]. Since the oxygen reduction is a structure-sensitive reaction, as revealed by the different activities for the reaction of the gold basal plane electrodes, the transition between the two mechanisms could be associated with the transition between the two different surface phases. At this point, the kinetics of the process of reconstruction/lifting of the reconstruction has to be considered. This process is generally regarded as slow, and a proof of this is the asymmetry of the voltammetric profiles in the supporting electrolytes (Fig. 4). On the Au(100) electrode, the peak in the positive scan at 0.26 V (SHE) in 0.1 M NaOH and at 0.5 V (SHE) in 0.1 M Na_2SO_4 is associated with the lifting of the reconstruction and there is no equivalent peak in the negative-going scan since the reconstruction process is slow. Although the rate of this process can be affected by the presence of different species in solution [13], in situ X-ray diffraction experiments reveal that the process of forming the reconstruction can be in the order of minutes to hours. If the process of reconstruction is responsible for the transition, the current recorded for oxygen reduction in positive and the negative scans would show a significant hysteresis, induced by the slowness of the reconstruction process. However, the curves in the positive- and negative-going scans (Figs. 2, 3, 4) have almost no hysteresis in the region where the transition takes place. Therefore, the

transition between the two surface mechanisms cannot be attributed to the surface reconstruction process. In situ STM [24] and X-ray [13] studies have demonstrated that the transformation between the (1×1) and the "hex" structure in not responsible for the change in the mechanism.

Another property that is linked to the position of the pzc is anion adsorption. Anions will remain adsorbed on the electrode surface at potentials positive to the pzc. Hydrogen peroxide has a $pK_a = 11.65$ for the first dissociation, and in basic solution the main species will be HO_2^-, as reflected in the mechanism for oxygen reduction. Therefore, at potentials positive to the pzc, HO_2^- will remain adsorbed and the reduction will proceed. At a given potential, negative to the pzc, this species will desorb effectively from the electrode surface and its reduction will not proceed further. The exact potential at which the desorption takes place will depend on the specific interaction between the surface and the HO_2^-. In fact, the presence of adsorbed HO_2^- in alkaline media on gold electrodes has been detected [25]. In acid media, the protonation mechanism will be faster and thus H_2O_2 will be directly formed, or if HO_2^- is formed it will be immediately react to yield H_2O_2 and be desorbed [7, 12].

If the specific adsorption of HO_2^- is the key parameter to yield OH^- as the final product, the presence of a strong adsorbing anion on the solution may compete with HO_2^- for the adsorption sites and force its desorption, hindering the reduction to OH^-. Figure 6 shows the results obtained in a phosphate buffered media (pH 7) and unbuffered sodium sulfate initially at pH 6. It is noteworthy that both waves develop in the same potential range, thus suggesting that the interfacial pH is not greatly affecting the reduction kinetics. As can be seen, phosphate adsorbs more strongly than sulfate, since the process of adsorption/desorption of the anion takes place at more negative potentials (Fig. 6A). Parallel to the stronger adsorption of phosphate, the reduction of oxygen starts at slightly more negative potentials. The maximum current obtained in phosphate media is significantly lower and the maximum value is equal to that obtained at −0.3 V in Na_2SO_4, i.e. the region where hydrogen peroxide is the final product. Therefore, the reduction of oxygen only yields hydrogen peroxide in phosphate media at pH 7, likely due to the competitive anion adsorption process.

When comparing the Au(100) electrode with the Au(111) surface, the latter electrode has a significantly lower catalytic activity for oxygen reduction (see Fig. 3) and also a higher pzc value. Assuming that the general behavior of the surface is the same as that of the Au(100) electrode, it can be seen that significant reduction currents on the Au(111) electrode are obtained in the region where the reduction on Au(100) yields only hydrogen peroxide. The difference between the catalytic activity for oxygen reduction of these electrodes has also been attributed to the different properties for OH adsorption on the electrodes [14]. Although the voltammetric

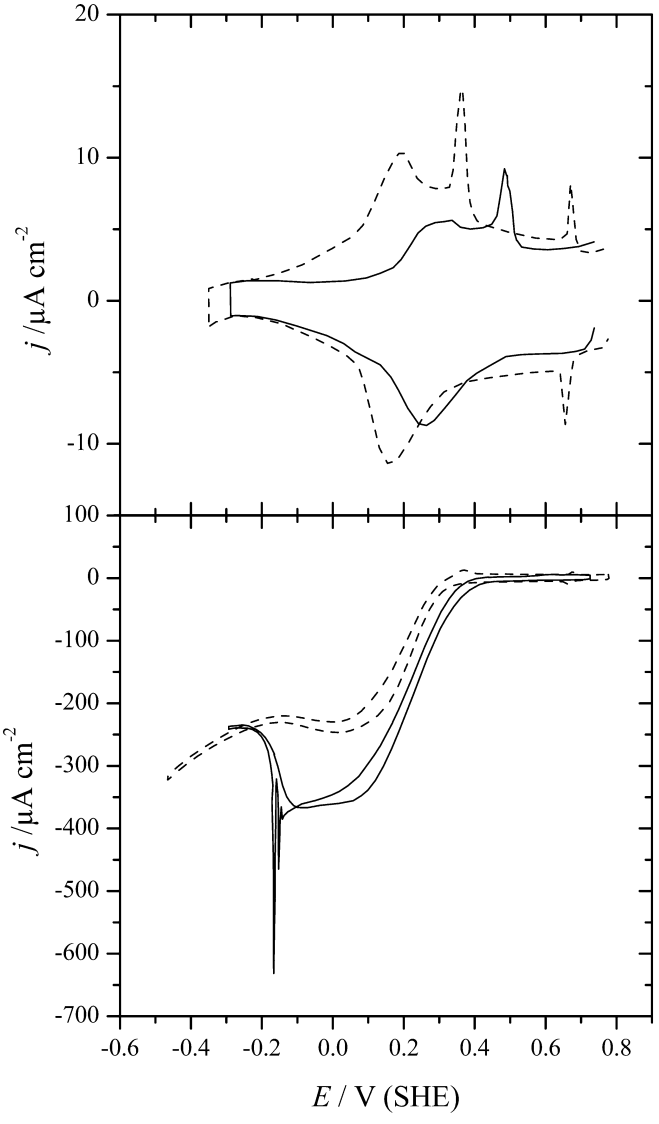

Fig. 6 *Top*: voltammetric profile for the Au(100) electrode in the double layer region in 0.1 M Na_2SO_4 (*full line*) and 0.1 M KH_2PO_4 + 0.1 M K_2HPO_4 0.1 M (*dashed line*) (scan rate 50 mV/s). *Bottom*: current densities measured for oxygen reduction in the impinging jet system in 0.1 M Na_2SO_4 (*full line*) and 0.1 M KH_2PO_4 + 0.1 M K_2HPO_4 (*dashed line*)

profiles of the electrodes in 0.1 M NaOH are different (Fig. 7), the amount of OH adsorbed in the region where the oxygen reduction takes place (below 0.2 V, see Fig. 3) is similar for both electrodes. Therefore, the differences in behavior for oxygen reduction cannot be univocally attributed to the ability of the surface to adsorb OH at the potentials at which oxygen reduction takes place, and have to be related to structural differences. Moreover, the reaction order for OH^- close to zero clearly indicates that OH^- is not involved in the reaction mechanism prior to the rate-determining step, implying that OH^- is not acting as catalyst.

The Au(110) electrode exhibits catalytic activity that has an intermediate value between the Au(100) and

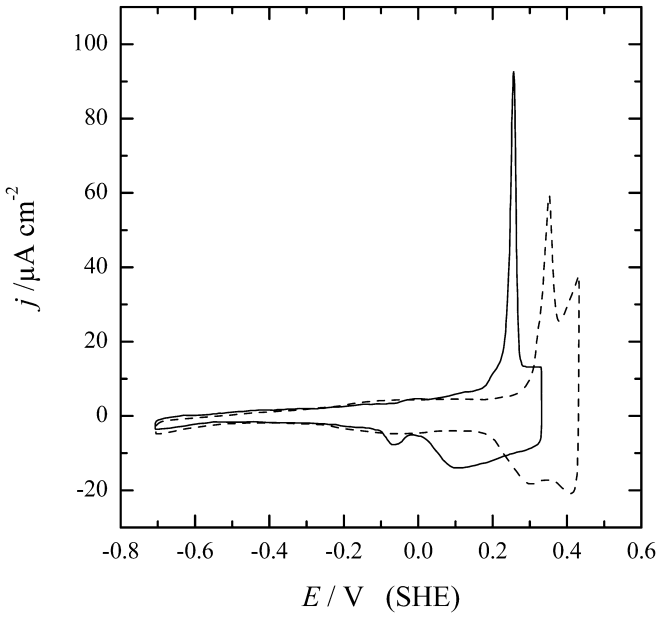

Fig. 7 Voltammetric profile in the double layer region for the Au(100) (*full line*) and Au(111) (*dashed line*) electrodes in 0.1 M NaOH (scan rate 50 mV/s)

Au(111) electrodes. This surface has the lowest pzc value of the three surfaces and also displays higher OH adsorption in the region where oxygen reduction takes place (see Fig. 1). Therefore, the highest catalytic activity of the Au(100) electrode has to be assigned to the specific interactions of the surface with the intermediate adsorption species (but not necessarily OH). In these interactions of the Au(100) electrode, both the geometrical arrangement and energies of the surface can play an important role, as has been postulated [14]. According to the behavior observed, the $4e^-$ mechanism is only followed when HO_2^- interacts with the (100) surface, i.e. there is a specific interaction of the Au(100) surface with HO_2^-, which is completely different from the other basal planes. This interaction ceases at potentials negative to the pzc.

Assuming that the reduction of oxygen to OH^- is linked to the ability of the surface to adsorb HO_2^-, a tentative model for the oxygen reduction on Au(100) can be proposed. The aim of this model is to reproduce the shape of the curve for oxygen reduction on this electrode in 0.1 M NaOH. In the experimental curve, two different regions can be distinguished. In the initial part (between 0.4 and 0.0 V SHE), the currents rise from zero to the value of a limiting diffusion current. In this region the final product is OH^-, and therefore four electrons are exchanged. The shape of this current region is associated with $4e^-$ transfer with mixed (diffusion/electron transfer) control. The equation describing this process is:

$$\frac{1}{j} = \frac{1}{j_{ex}} + \frac{1}{j_{dif}} = \frac{1}{-j_o \exp\left(-\frac{\alpha_c nF}{RT}\left(E - E_{eq}\right)\right)} + \frac{1}{-4Fk_d c_{O_2}} \tag{4}$$

where j_o is the exchange current density for the oxygen reduction process, α_c is the cathodic electronic transfer coefficient, E_{eq} is the equilibrium potential for the process (1.23 V vs. RHE), k_d is the mass transfer coefficient (which depends on the diffusion coefficient and the Nernst diffusion layer) and c_{O_2} is the oxygen concentration in solution. Since the Tafel slope for the process is 120 mV, $n\alpha_c$ should be equal to 0.5.

Within the second region (between 0.0 and −0.4 V vs. RHE), the process is controlled by diffusion, but the mechanism changes from four-electron transfer (OH^- as a final product) at potentials above −0.2 V (RHE) to two-electron transfer (hydrogen peroxide) at potentials below −0.2 V. The final number of electrons exchanged is associated with the ability of the surface to adsorb HO_2^-. For potentials at which HO_2^- is adsorbed, four electrons are exchanged. The surface coverage of HO_2^- can be assumed to follow a Frumkin isotherm:

$$\frac{\theta}{1-\theta} = K_{ads} c_{HO_2^-} \exp(fE) \exp(gf\theta) \tag{5}$$

where K_{ads} is the adsorption constant for the process, $c_{HO_2^-}$ is the concentration in the Helmholtz plane of HO_2^- (which can be considered constant), and g is the interaction parameter. When θ is close to 1, four electrons are exchanged, whereas only two electrons are exchanged when $\theta = 0$. Therefore, the number of electrons exchanged in the process can be written as:

$$n = 2 + 2\theta \tag{6}$$

and the limiting current in this region has a value of:

$$j_2 = (2 + 2\theta) F k_d c_{O_2} \tag{7}$$

To evaluate the current in this region, the HO_2^- coverage as a function of the potential is calculated according to Eq. 5 and this value is substituted in Eq. 7. In order to compare the experimental and theoretical data, the current densities have been normalized to the maximum current density obtained at −0.1 V (SHE). The results are plotted in Fig. 8, for a case in which $g = 1$, $K_{ads} c_{HO_2^-} = 3$ and $k_d/j_o = 40$. As can be seen, the model reproduces the shape of the curve, especially in the region where the transition of the mechanisms takes place. Therefore, the ability of the surface to adsorb HO_2^- could justify the differences of behavior found for the different basal planes for oxygen reduction and the change of mechanism observed in basic and neutral media for the Au(100) electrode.

Regarding the presence of oscillations, they only appear in the negative-going scan in the region where the transition between the two- and four-electron oxidation mechanisms takes place. The oscillations are linked to the HO_2^- reduction since the oscillations are also present at the same potential when hydrogen peroxide is reduced to OH^- on a Au(100) electrode in 0.1 M NaOH [26]. The transition between the two mechanisms takes place in a narrow potential region, and the currents correspond to the limiting diffusion current for the two mechanisms.

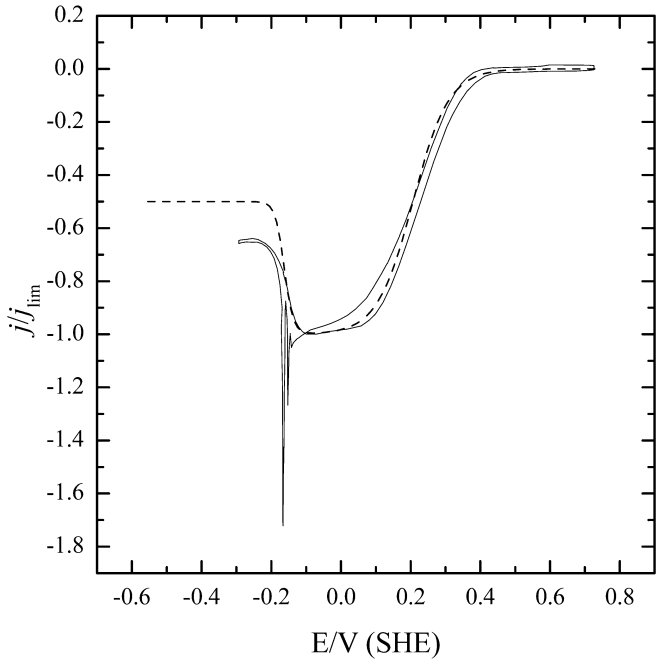

Fig. 8 Comparison of the normalized current densities (j/j_{lim}) for the Au(100) electrode in 0.1 M Na_2SO_4 (*full line*) and the currents predicted by Eq. 7 (*dashed line*)

However, the maximum current in the oscillation is higher than the limiting diffusion current for the four-electron mechanism. Similar oscillations have been observed for H_2O_2 reduction on silver electrodes in acidic media using rotating disk electrodes [27]. The presence of such oscillations has been attributed to the difference between the applied potential and the electrode potential together with the diffusion dynamics of the implied species. Owing to the similarities between the current responses in both cases, the presence of oscillations also has the same origin.

Acknowledgements This work was supported by the Spanish DGI through project no. BQU2000-0240 and by the European Union Framework V Growth Programme, CLETEPEG project, contract no. G5RD-CT-2001-00463.

References

1. Tarasevich MR, Sadkowsky A, Yeager E (1983) Oxygen electrochemistry. In: Conway B, Bockris JO'M, Yeager E, Khan SUM, White RE (eds) Comprehensive treatise of electrochemistry, vol 7. Plenum, New York, pp 301–398
2. Schiffrin DJ (1983) The electrochemistry of oxygen. In: Pletcher D (ed) Electrochemistry, vol 8. (Specialist periodical reports) Royal Society of Chemistry, London, pp 126–170
3. Kinoshita K (1992) Electrochemical oxygen technology. Wiley, New York
4. Adzic R (1998) Recent advances in the kinetics of oxygen reduction. In: Lipkowsky J, Ross PN (eds) Electrocatalysis. VCH, New York, pp 197–242
5. Anastasijevic NA, Vesovic V, Adzic RR (1981) J Electroanal Chem 229:305
6. Anastasijevic NA, Vesovic V, Adzic RR (1981) J Electroanal Chem 229:317
7. Alvarez-Rizzati M, Juttner K (1982) J Electroanal Chem 144:351
8. Adzic RR, Markovic NM (1982) J Electroanal Chem 138:443
9. Adzic RR, Markovic NM, Vesovic VB (1984) J Electronal Chem 165:105
10. Adzic RR, Markovic NM, Vesovic VB (1984) J Electronal Chem 165:121
11. Anastasijevic NA, Strbac S, Adzic RR (1988) J Electroanal Chem 240:239
12. Strbac S, Anastasijevic NA, Adzic RR (1992) J Electroanal Chem 323:179
13. Polewska W, Vitus CM, Ocko BM, Adzic RR (1994) J Electroanal Chem 364:265
14. Strbac S, Adzic RR (1996) J Electroanal Chem 403:169
15. Bergelin M, Wasberg M (1998) J Electroanal Chem 449:181
16. Clavilier J, Armand D, Sun DG, Petit M (1986) J Electroanal Chem 205:267
17. Strbac S, Hamelin A, Adzic RR (1993) J Electroanal Chem 362:47
18. Strabac S, Adzic RR (1996) Electrochim Acta 41:2903
19. De Moraes IR, Nart FC (1999) J Electroanal Chem 461:110
20. Hamelin A (1995) J Electroanal Chem 386:1
21. Gao X, Edens GJ, Weaver MJ (1994) J Electroanal Chem 365:47
22. Kolb DM (1996) Prog Surf Sci 51:109
23. Bohnen KP, Kolb DM (1998) Surf Sci 407:L629
24. Markovic NM, Tidswell IM, Ross PN (1994) Langmuir 10:1
25. Wu B-L, Lei H-W, Cha C-S, Chen Y-Y (1994) J Electroanal Chem 377:227
26. Strbac S, Adzic RR (1992) J Electroanal Chem 337:335
27. Flätgen G, Wasle S, Lübke M, Eickes C, Radhakrishnan G, Doblhofer K, Ertl G (1999) Electrochim Acta 44:4499